SRYAHWA PUBLICATIONS

Annals of Archaeology
ISSN: 2639-3662 | Volume 8, Issue 1, 2026
https://doi.org/10.22259/2639-3662.0801001

RESEARCH ARTICLE

Why Blood Stains on the Turin Shroud are of Red Colours? Optical Microscopy Studies and SEM-EDX Analyses

Gérard Lucotte

Institute of Molecular Anthropology, Paris, France.

Received: 23 January 2026 Accepted: 10 February 2026 Published: 17 February 2026

Corresponding Author: Gérard Lucotte, Institute of Molecular Anthropology, Paris, France.

Abstract

We review here previous and actual results concerning sixty-nine particles and sub-particles located at the surface of a sample of the Turin Shroud taken in a blood stain of the Face. These artificial products (nine hematites, nine biotites, one cinnabar, fifteen iron rich clays, eight particles of iron oxides, eleven miniums and sixteen particles of potassium alumina silicate with iron) are of potentially red colours. We explain the red colour of the sample by the intentional addition of these products during time, as a reinforcement of the faded red blood cells colour on this ancient linen time.

Keywords: Turin Shroud, Face Area, Blood Stains, Red Colours, Iron Oxides, Optical Microscopy, Scanning Electron Microscopy, Energy Dispersive X-Ray.

1. Introduction

The Turin Shroud (TS) is a well known ancient linen tissue on which a body image is imprinted (12). The body and the head of this image are covered by numerous blood stains. In fact there are at least two interpretations of these blood stains of red-brown colours : the first interpretation was given by Heller and Adler (3, 4), that made numerous efforts to explain red blood as a mixture between bilirubin and an exotic complex of oxidised met-hemoglobin of red blood cells. At that time Mc Crone (11), on the basis of polarized light microscopy studies of the TS particles, established that this red-brown colour was mainly due to aggregates of crystalline particles of hematite (an iron-oxide mineral) and vermilion (a painting constituted of cinnabar mineral).

I have obtained a small triangular sticky tape that was sampled on the TS surface, corresponding to a part of the Face of this body, and we concentrated in the past years on the study of microscopic particles located on the surface of this sticky tape (7). SEM-EDX analyses of this sample permits us to detect twenty-five corpuscules (or corpuscule groups) that are human red blood cells (6) according to morphological and chemical criterias ; but, according to optical microscopy studies, only two of them (h19 : the e22 particle, and h22 : the g25 particle) are of red colour.

We have previously studied red-colour particles on the triangle surface, including two hematite, nine biotite and one cinnabar particles (9) ; more recently we studied on this surface fifteen iron-rich clays. In the present study I describe seven other hematite particles and several particles of iron oxides, of miniums and potassium alumino-silicates with iron.

2. Material and Methods

The material is the small (1.36 mm height, 614 µm wide) sticky tape triangle at the surface of which all particles were deposited. This sample was taken in a blood stain of the face. In optical microscopy the triangle appears of red colour, with variable intensities among the areas (the more reddish intensity is in the central part of the triangle). For practical reasons, the surface of the triangle was subdivided into nineteen sub-sample areas, named A to S ; because of its complexity, the E area was subdivided into seven (a to g) sub-areas. The three samples of reference are : an

Citation: Gérard Lucotte. Why Blood Stains on the Turin Shroud are of Red Colours? Optical Microscopy Studies and SEM-EDX Analyses. Annals of Archaeology. 2026;8(1): 01-16.

hematite stone, from my personal mineral collection ; a minium powder, from Sennelier, Paris ; a red ochre pigment (from "le comptoir des ocres", Apt, France).

The particles studied were previously observed (to determine colour) by optical microscopy (both direct and inverted views of the triangle), using a photo-microscope Zeiss (Model III, 1972).

These particles were also observed, with any preparation, on the adhesive part of the triangle. These observations were conducted by SEM (Scanning Electron Microscopy), using a Philips XL instrument (of the environmental version). GSE (Gazeous Secondary Electrons) and BSE (Back Scattering Electrons) procedures were used, the second one to better detect heavy elements. Elemental analyses for each particle observed were realized by EDX (Energy Dispersive X-ray), this SEM1 microscope being equipped with a Bruker probe AXS-EDX (the system of analysis is PGT : Spirit Model of Princeton Gamma Technology).

Particles b27, b28 and b28', p19, k19 and the red ochre pigment of reference were examined with another SEM apparatus (SEM2) : a FEI Model Quanta 25 of FEG, both in LFD (Large Field Detector) and CBS (Circular Back Scattering) procedures.

The minium powder of reference was studied by a third apparatus (SEM3), an Auriga FEG-FIB (Zeiss), images being performed in secondary electrons.

Each elemental analysis is given in the form of a spectrum, with kiloelectrons/Volts (ke/V) on the abscissa and elemental peak heights in ordinates. Highly Resolutive (HR) spectras are those where the ordinate graduations are enhanced, to better see little peaks.

For hematites and other particles, elemental compositions are given, values being studied on the main elemental peaks (of oxygen and iron).

3. Results

We have found on the surface of the triangle seven new hematites. Other new particles found on this surface are several iron oxides, miniums and potassium alumino-silicates with iron.

Seven supplementary hematites (b27, b28 and b28', b35, b36, b37 and i14) are detected on the triangle surface. SEM photograph of **Figure 1** shows some part of the B area of the triangle near the right border containing b27, b28 and b28' particles. Other particles in this area are : b21 and b21', two ceramics; b26, a clay with iron ; b29, a clay iron-rich with barium sulphate and cadmium sulphure ; b39, a silica ; b40, an illite with iron ; b41, a feldspath). The b28, b28' and b27 particles are triangular, with maximal lengths of about 14 µm, 4 µm and 3 µm respectively. Spectras of b27 and b28 are characteristics of hematite (the b28' spectrum is the same that of b28, but the b28 spectrum indicates an important calcification). Because of the proximity of the right border of the triangle, particles b27, b28 and b28' cannot be seen in optic microscopy.

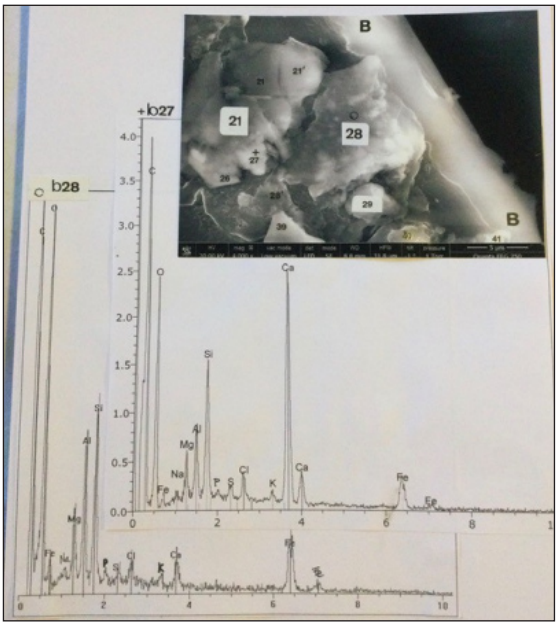

Figure 1. *The b27, b28 and b28' particles. Above : SEM2 photograph (4 000x), in LFD, of some part of the B area near the right border of the triangle showing b27, b28 and b28' (B : triangle border ; + and O : approximate region where the SEM-EDX analyses are realized). Lower spectrum : that of b28. Upper spectrum : HR spectrum of b27. C : carbon ; O : oxygen ; Fe (three peaks) : iron ; Na : sodium ; Mg : magnesium ; Al : aluminium ; Si : silicium ; P : phosphorous ; S : sulphur ; Cl : chlorine ; K : potassium ; Ca (two peaks) : calcium.*

SEM photograph of **Figure 2** shows some other part of the B area containing b35, b36 and b37. Other particles in this area are : b33, a smectite ; b34 is covered by calcium carbonate ; b35', a calcium carbonate ; b38, a silica ; b43, a peridot ; b47, a gypsum ; b48, which is organic ; b49, a quartz. The b35, b36 and b37 particles are oval, with maximal lengths of about 12 µm, 10 µm and 28 µm, respectively. Spectrum of b36 is that of an hematite, with calcification. Optical photograph of the area shows that particles b35 and b37 are brown and particle b36 is clear-red. **Figure 3** shows spectras of b35 and b37 ; both are characteristics of hematite, with calcification.

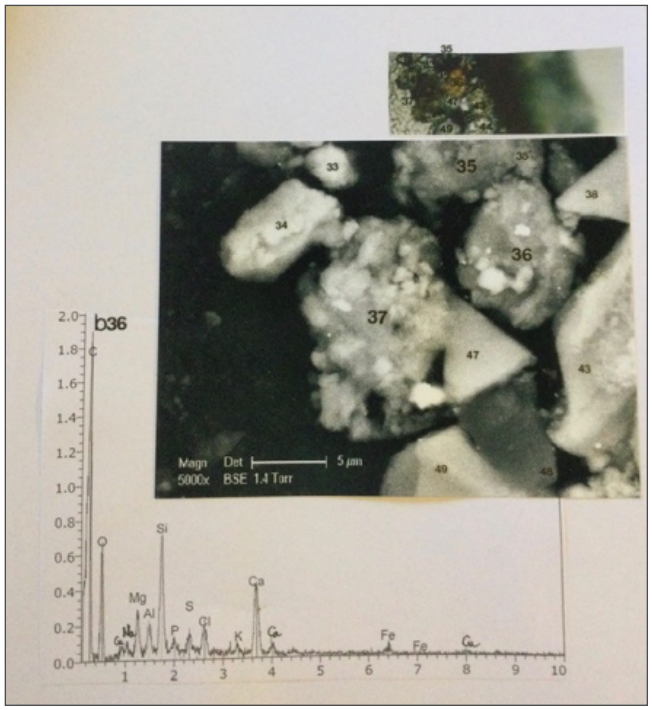

Figure 2. *The b35-35', b36 and b37 particles. Lower photograph : SEM1 photograph (5000x), in BSE, of some other part of the B area containing b35-35', b36 and b37. Upper photograph : optical microscopy photograph (1200x) of that area. Below : the HR spectrum of b36. Cu (two peaks) : copper.*

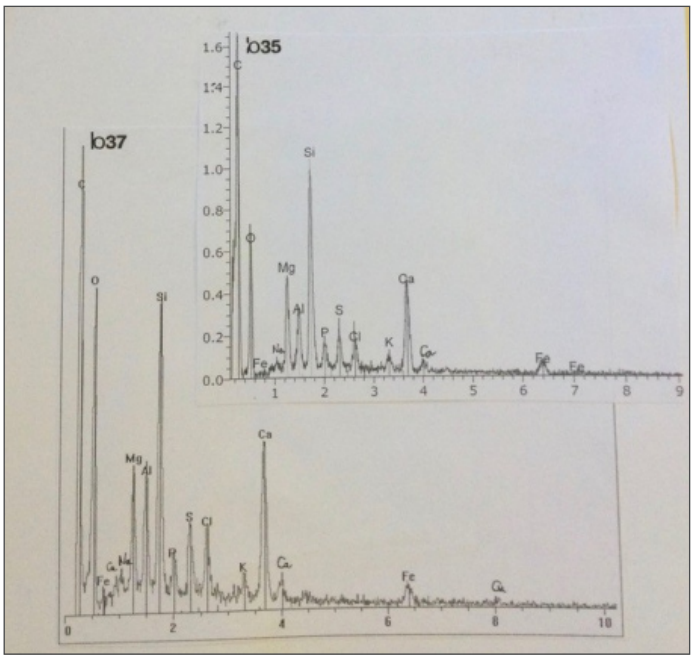

Figure 3. *Spectras of b35 (above) and of b37 (below).*

SEM photograph of **Figure 4** shows some part of the I area containing i14. Other particles in this area are i14 (an Ostracod) and i15 (a glass). The i14 particle is triangular, with an approximate length of about 12 µm. Its spectrum is characteristic of hematite. The enlarged optical view of that area shows that the i14 colour is brown-red.

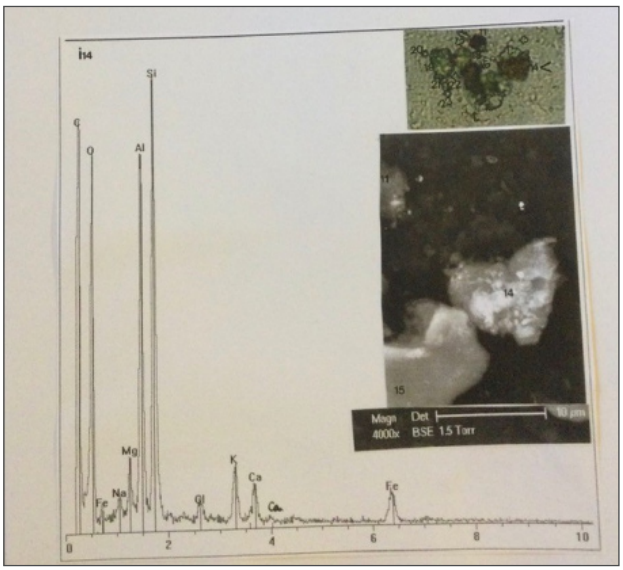

Figure 4. *The i14 particle. Lower photograph : SEM1 photograph (4 000x), in BSE, of some part of the I area containing i14. Upper photograph : enlarged optical microscopy photograph (1200x) of that area. Below : the spectrum of i14.*

Table 1. *List and characterisation of the seven new hematite particles.*

Numbers	Nomenclature	Areas	Forms	Maximal lengths (in µm)	Hematite spectras	Peculiarities	Colours
1	b27	B	triangular	3	+	Ca↗	Not visible
2	b28		triangular	14	+		not visible
3	b28’		triangular	4	+		not visible
4	b35		oval	12	+	Ca↗	brown
5	b36		oval	10	+	Ca↗ ; Cu	clear-red
6	b37		oval	28	+	Ca↗ ; Cu	brown
7	i14	I	triangular	12	+		brown-red

3.1 Iron Oxyde Particles

The spectrum of **Figure 5** is that of an iron oxide sample of reference. It shows a very elevated main peak of iron and an elevated peak of oxygen. Normal composition of this sample shows percentages of 77.96% of iron and of 22.04% of oxygen.

Eight iron oxide particles are detected on the triangle surface : a5, “i1”, “i2”, i61, j31, l70, p9 and p19.

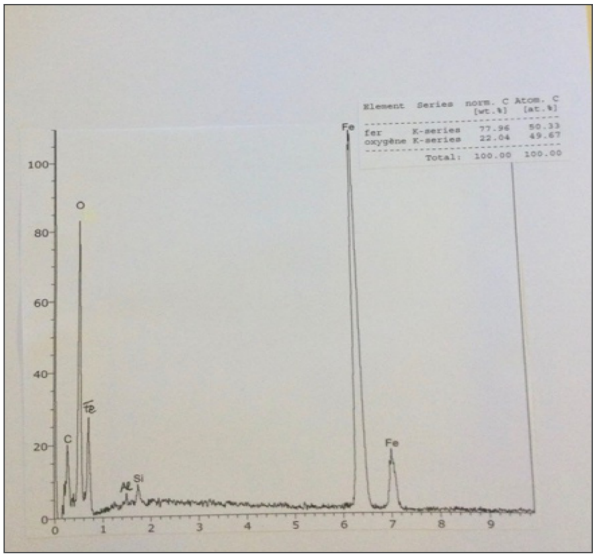

Figure 5. *Spectrum of an iron oxide sample of reference. Insert : normal composition of the sample (fer : iron ; oxygène : oxygen).*

Figure 6 shows an inverted view in optic microscopy showing areas A and B of the triangle. The a5 particle, visible at the naked eye, is rounded and of red-brown colour ; it was initially considered as a potential red blood cell.

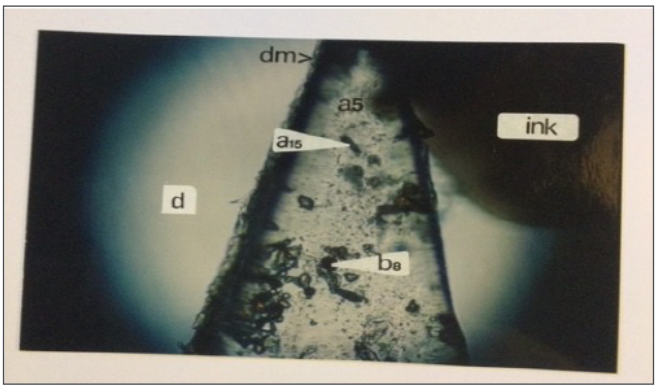

Figure 6. *Optical microscopy photograph (1200x) of an inverted view of the glass where part of the triangle (A and B areas) was stuck, showing the a5 particle (d : right side ; dm : right border ; ink : black in mark ; a15 : a titanium micro-segment ; b8 : a red clay).*

The SEM photograph of **Figure 7** shows some part of the A area containing the a5 particle ; its maximal dimension is of about 15 µm. Its spectrum is characteristic of an iron oxide.

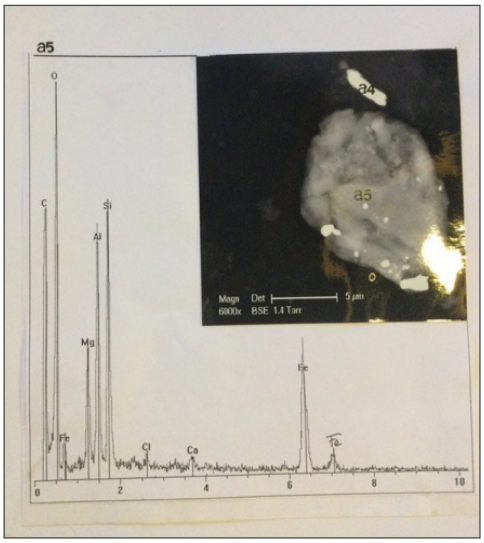

Figure 7. *The a5 particle. Above : SEM1 photograph (6000x), in BSE, of some part of the A area showing a5 (a4 : a little micro-blade of iron). Below : the a5 spectrum.*

The SEM photograph of **Figure 8** shows some part of the ß area containing the "i1" and "i2" particles. Other particles in this area are : b20, with multiple elements ; b22, with gold ; b23 and b25, both calcium carbonates ; b21, a steatite ; b26, a clay ; FL3 is the third linen fibre fragment. Particles "i1" and "i2" are particle fragments, with angular outlines and of about 1 µm of maximal dimensions. Their spectras are characteristic of iron oxides. Because of their little dimensions, their colours cannot be seen in optical microscopy.

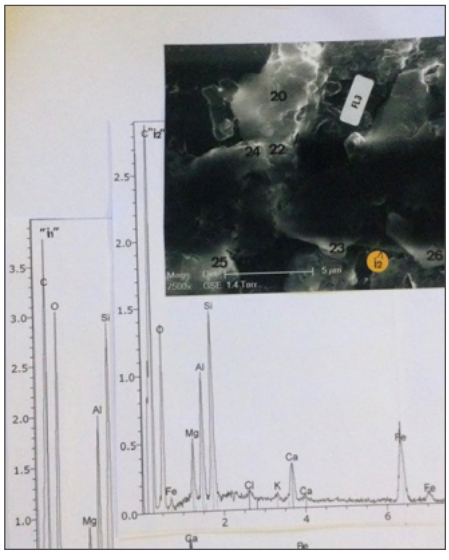

Figure 8. *The "i1" and "i2" particles. Above : SEM1 photograph (7500x), in GSE, of some part of the B area containing "i1" and "i2". Below : HR spectras of "i1" and "i2".*

The middle SEM photograph of **Figure 9** shows some part of the I area containing the i61 particle. Other particles in this area are : i59, a montmorillonite (8) ; i60, a feldspath ; i62, a steatite ; i63, a kaolinite. The i61 particle is rounded and of maximal dimension of about 11 µm. Its spectrum is characteristic of an iron oxide. Its colour is yellow-red in optic microscopy.

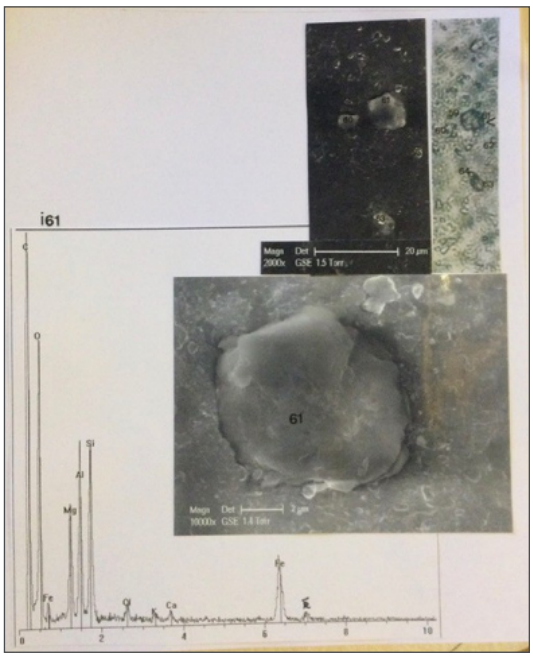

Figure 9. *The i61 particle. Above : left photograph : SEM1 photograph (2 000x), in GSE, of some part of the I area containing i61 ; right photograph : optical microscopy photograph (1200x) of that area part. Middle : SEM1 photograph (10000x), in GSE of the part of the I area with i61. Below : the i61 spectrum.*

Figure 10 shows SEM photographs of some part of the J area containing the j31 particle. Other particles in this area are : j32, a Cyanophycae ; j33, a calcium carbonate ; j34, a lapis lazuli ; j27, a triangular Diatom. The j31 particle is triangular, with about 7 µm of height. Its colour is red.

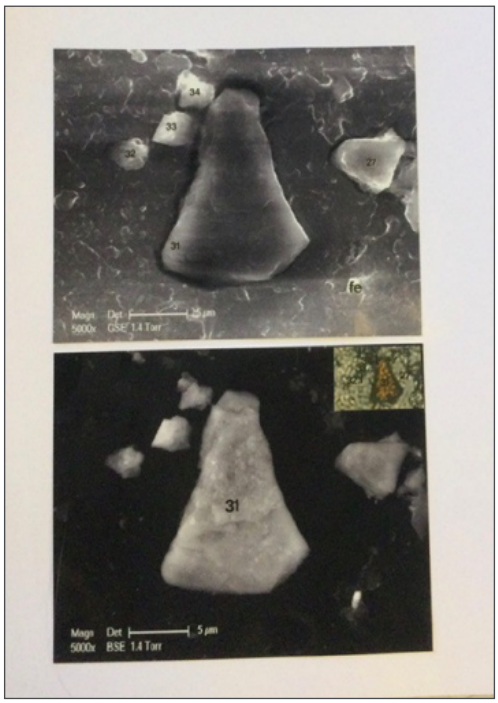

Figure 10. *The j31 particle. Above. SEM1 photograph (5 000x), in GSE, of some part of the J area containing j31 (Fe : a micro-particle of iron). Below : SEM1 photograph (5000x), but in BSE, of this area. Insert : optical miscroscopy photograph (1200x) showing j31.*

The spectrum of **Figure 11** is that of j31 ; it is that of a characteristic iron oxide (where manganese accompanies iron, that proving the mineral origin of iron). The normal composition of j31 shows a percentage of iron of 43.88%.

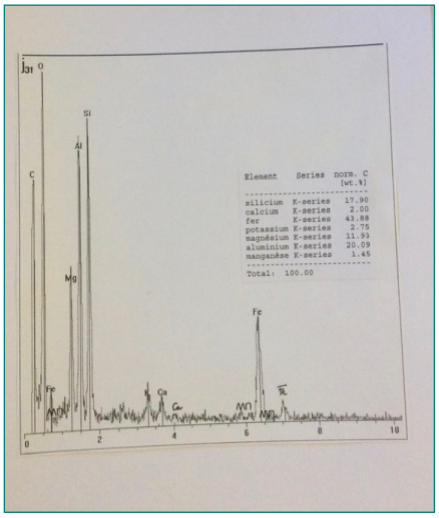

Figure 11. *The j31 spectrum. Insert : normal composition of the sample (fer : iron, magnésium : magnesium ; manganèse : manganese). Mn (two peaks) : manganese.*

The SEM photograph of **Figure 12** shows some part of the L area containing l70. Other particles in this area are : l64, a potassium alumino silicate with iron ; l65 a Coccolith ; l68, a biotite (l72 is a hole). The j31 particle is triangular, with about 5 µm of height. Its colour is red-brown. Its spectrum is that of an iron oxide.

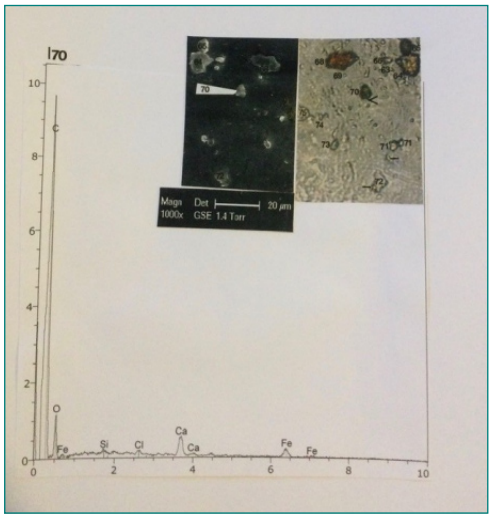

Figure 12. *The l70 particle. Left photograph : SEM1 photograph (1000x), in GSE, of some part of the L area containing l70. Right photograph : an inverted view of an optical microscopy photograph (1200x) of this area. Below : the l70 spectrum.*

The SEM photograph of **Figure 13** shows some part of the P area containing the p9 particle. Other particles in this area are : p7, a marble ; p8, a Cyanophycae ; p10, a potassium alumino-silicate with iron ; p11 and p12, two lapis lazuli ; p13, a steatite ; p14, a phosphate ; p15, a pigment ; p16, a quartz.

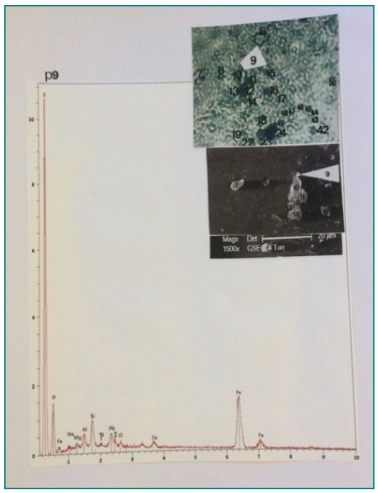

Figure 13. *The p9 particle. Lower photograph : SEM1 photograph (1500x), in GSE, of some part of the P area containing p9. Upper photograph : optical microscopy photograph (1200x) of this area. Below : the HR spectrum of p9. Pb : lead.*

The p9 particle is a micro-ball, of about 2 µm of diameter. Its spectrum is characteristic of an iron oxide. Its colour is pale red. The SEM photograph of **Figure 14** shows another part of the P area containing p19. Other particles in this area are : p18, a calcite ; p22, a steatite ; p23, a biotite ; p24, a jay ; p42 is organic. The p19 particle is rounded, with about 4 µm of maximal length. Its colour is pale red. Its spectrum is characteristic of an iron oxide (the normal composition of p19 shows a percentage of iron of 87.15%).

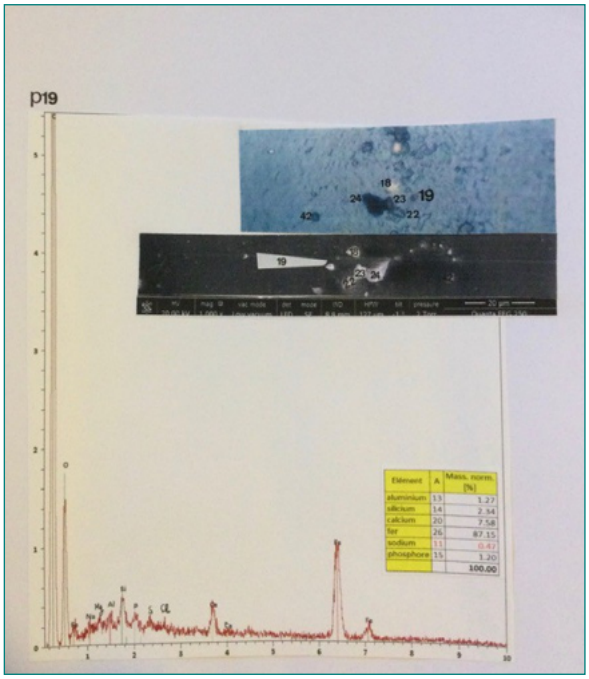

Figure 14. *The p19 particle. Lower photograph : SEM2 photograph (1 000x), in LFD, of some part of the P area containing p19. Upper photograph : optical microscopy photograph (1200x) of that area. Below : the HR spectrum of p19. Insert : normal composition of the sample (fer : iron ; phosphore : phosphorous).*

Table 2. *List and characterization of the eight iron oxide particles*

Numbers	Nomenclature	Areas	Forms	Maximal lengths (in µm)	Iron oxide spectras	Peculiarities	Colours
1	a5	A	rounded	15	+		red-brown
2	"i1"	B	angular	1	+	Ca↗	not-visible
3	"i2"		angular	1	+	Ca↗	not-visible
4	i61	I	rounded	11	+		yellow-red
5	J31	J	triangular	7	+	Mn	red
6	l70	L	triangular	5	+		red-brown
7	p7	P	micro-ball	2	+		pale red
8	p19		rounded	4	+		pale red

3.2 Minium Particles

Minium is a lead tetroxide, of chemical formula Pb_3O_4. It is a red orangey pigment that was used in painting. **Figure 15** summarizes results obtained on a powder of modern minimum of reference. The SEM photograph of this figure is a part of this powder, composed of particles of more than 6 µm of maximal lengths ; colour of the powder is intense red. The global spectrum of the powder shows elevated peaks of oxygen and of the lead mean peak.

There are one formation, a5 (1-7) and four particles (j64, p37, p41 and q6) of minium detected on the triangle surface.

The SEM photograph of **Figure 16** shows some part of the A area where the a5 particle is located. This particle is covered by at least seven sub-particles (1-7) of minium ; sub-particle **1** is rounded and of about 1 µm of diameter, sub-particle **4** is quadrangular and of about 3 µm of maximal dimension, and sub-particles **2**, **3**, **5-7** are micro-balls of less than 1 µm of diameter. They appear, in optical photography (for the most important ones) as red spots on the red-brown colour of the a5 particle. Spectras of **1** and **4** are those of miniums. So, the a5 (1-7) formation appears as minim painting remains on the a5 surface.

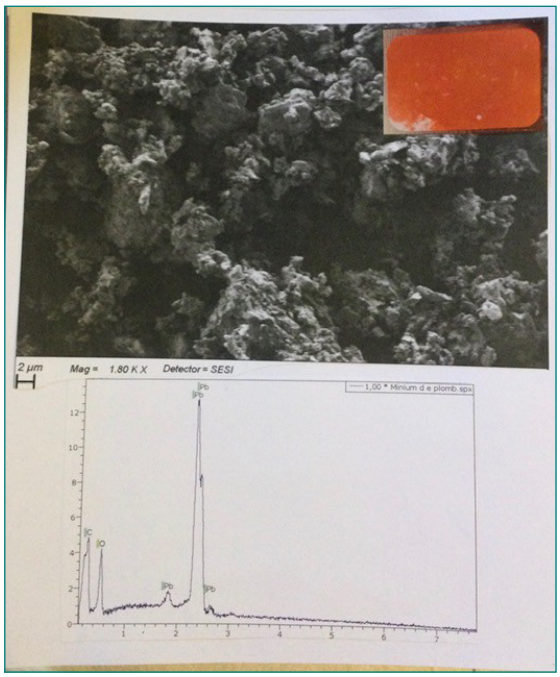

Figure 15. *Study of the minium sample powder of reference. Above : SEM3 photograph (1800x) of some part of this powder. Insert : optical microscopy photograph of the powder. Below : global spectrum of the powder. Pb (four peaks) : lead.*

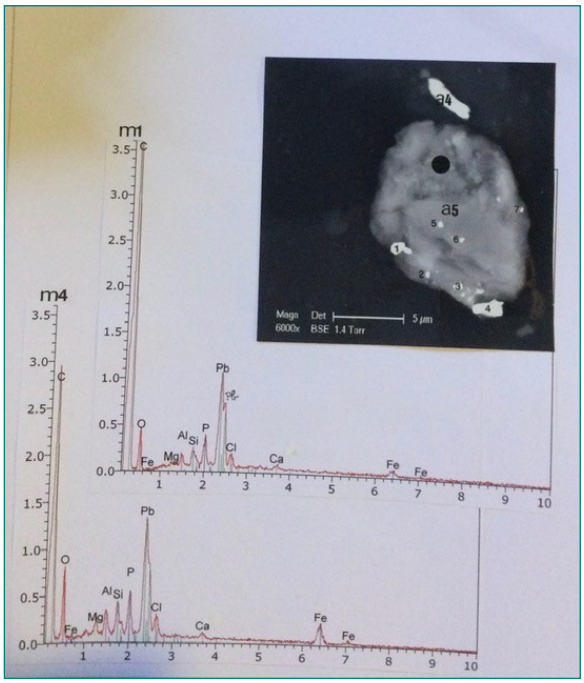

Figure 16. *The a5 (1-7) formation. Above : SEM1 photograph (6000x), in BSE, of some part of the A area containing a5 (a4 : an iron oxide micro blade ; 1-7 : sub-particles of minium ; the black spot on a5 indicates the approximate location where SEM-EDX analysis of 5 was realized). Below : HR spectras of sub-particles m1 and m4.*

The SEM photograph of **Figure 17** shows some part of the J area containing the j64 particle. Other particles of this area are : j56, a triangular Diatom, j57 a Dinophycae ; j62, a calcium carbonate ; j63, a Cyanophycae ; j63', a micro-blade of iron ; j65, a Dinophycae ; j66, a lapis lazuli. The j64 particle is rounded and of about 3 µm of diameter. Its colour is pale red. The j64 spectrum corresponds to that of a minium.

The SEM photograph of **Figure 18** shows some part of the P area containing the p37 and p41 particles. Other particles in this area are : p18, a calcite ; p19, the iron oxide ; p22, a steatite ; p23, a biotite ; p26, a glass ; p27, a steatite ; p28, a Cyanophycae ; p32, a potassium alumino-silicate with iron ; p33, a gypsum ; p35, an Ostracod ; p38, a spore ; p39, a pigment ; p40, a calcium phosphate. The p37 particle is a micro-ball, of less than 1 µm of diameter ; its colour is pale yellow. The p41 is ovale, with about 4 µm of maximal dimension ; its colour is pale red. The p37 and p41 spectras are those of miniums.

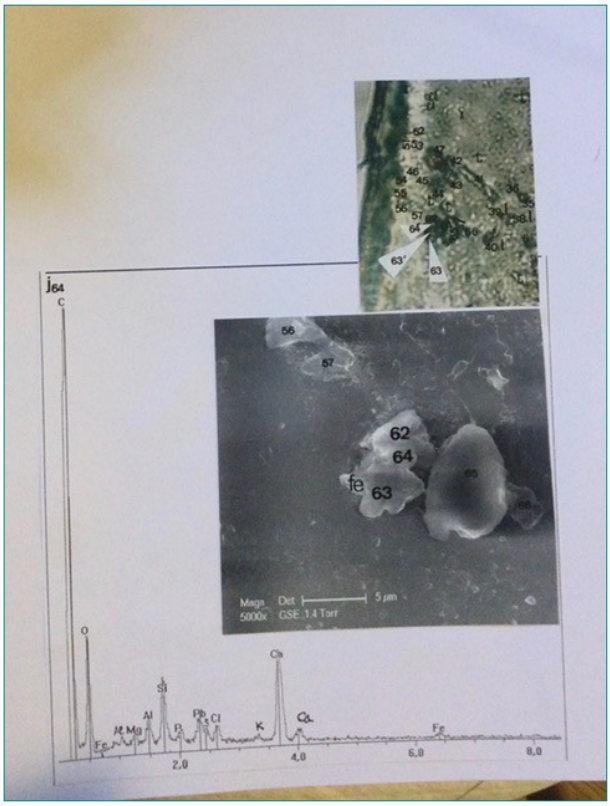

Figure 17. *The j64 particle. Lower photograph : SEM1 photograph (5 000x), in GSE, of some part of the J area containing j64. Upper photograph : optical microscopy photograph (1200x) of that area. Below : the j64 spectrum.*

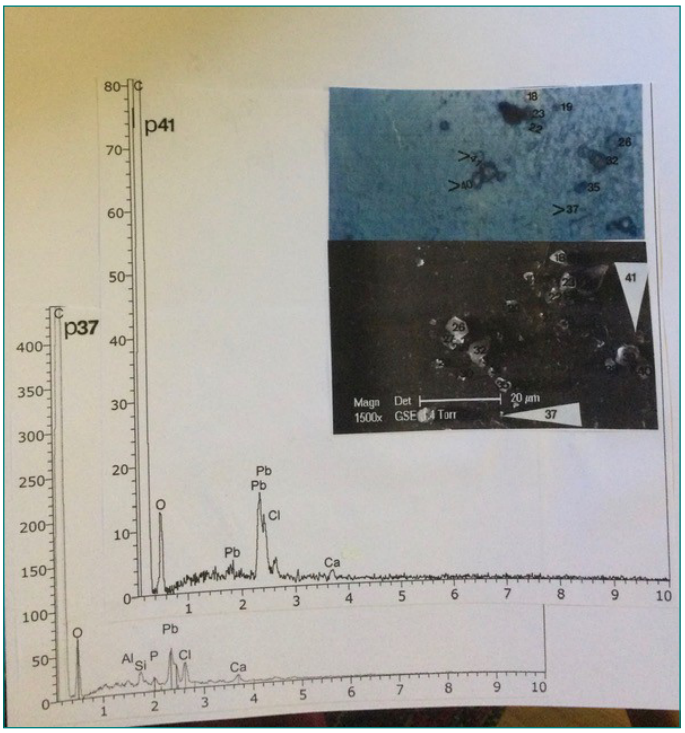

Figure 18. *The p37 and p41 particles. Lower photograph : SEM1 photograph (1 500x), in GSE, of some part of the P area showing p37 and p41. Upper photograph : inverted optical microscopy photograph (1200x) of that area. Below : the HD spectras of p37 and p41.*

The SEM photograph of **Figure 19** shows the Q area containing the q6 particle. Other particles in this area are : q1, a montmorillonite ; q2, a mixture of calcium carbonate and lapis lazuli ; q3, a marble micro fragment ; q4, a mixture of lapis lazuli and jay ; q5, a double carbonate ; q7, a pollen ; q8, a Coccolith ; q9, a peculiar micro-ball of iron ; q10 : a calcium carbonate ; q11, a modern glass ; q12, a complex pigment ; q13, a marble micro-fragment ; q14, a double carbonate ; q15, a gypsum. The q6 particle is ovale, with a maximal dimension of about 4 µm. Its colour is red. The q6 spectrum contains minium, with sodium, chloride, iron, barium sulphate and copper.

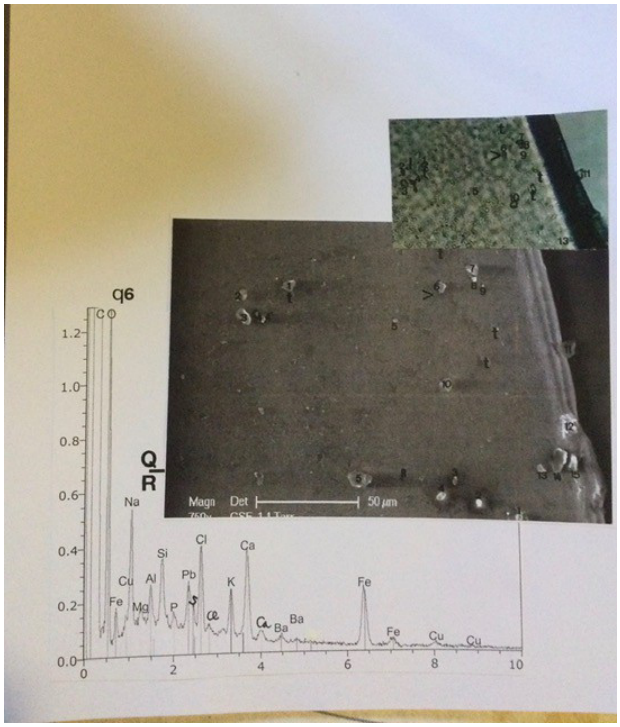

Figure 19. *The q6 particle. Lower photograph : SEM1 photograph (760x), in GSE, of the Q area containing q6 (R : upper limit of the R area ; t : holes). Upper photograph : optical microscopy photograph (1200x) of that area. Below : the HR spectrum of q6. Ba (two peaks) : barium.*

Table 3. *List and characterisation of the minium formation and of the four particles of minium.*

Numbers	Nomenclature	Areas	Forms	Maximal lengths (in µm)	Minium spectras	Peculiarities	Colours
1	a5(1-7) **1**	A	rounded	1	+		red-brown
	2		micro-ball	<1	+		not visible
	3		micro-ball	<1	+		not visible
	4		quadrangula	3	+		red- brown
	5		micro-ball	<1	+		not visible
	6		micro-ball	<1	+		not visible
	7		micro-ball	<1	+		not visible
2	j64	J	rounded	3	+	Ca↗	pale red
3	p37	P	micro-ball	<1	+		pale yellow
4	p41		ovale	4	+		pale red
5	q6	Q	ovale	4	+	ClNa, $BaSO_4$,Fe, Cu	red

3.3 Particles of Potassium Alumino-Silicate With Iron

These particles are clay-derived materials such as Portland cement and other dusts of the soil resulting from products of construction (5). They have peculiar spectras, with potassium and iron and very elevated values of aluminium, of silicium and of oxygen. Their colours are generally red depending on their iron contents. Particles l14, l17, l21 and l26 were previously identified as brick fragments (9).

Sixteen particles of potassium alumino-silicate with iron are detected on the triangle surface : a24, b78, d13, e113, j30, k59, l58, l64, l72, m15, m54, p6, p10, p32, q17 and r13.

As an example of particle of potassium alumino-silicate with iron, the SEM photograph of **Figure 20** shows some part of the K area containing the k59 particle. Other particles in this area are : k57, a calcite ; k58, a spore ; k60, a phosphorite ; l6, a calcite ; l7, a montmorillonite. The k59 particle is elongated, with 10.8 µm of maximal dimension. Its colour is yellow-red. Its spectrum is characteristic of those of potassium alumino-silicate particles with potassium peaks, with very elevated silicium and aluminium peaks ; the iron content is low, that explaining the yellow-red colour.

The m15 spectrum of **Figure 21**, with elevated content of iron oxide, explains the red colour of this particle.

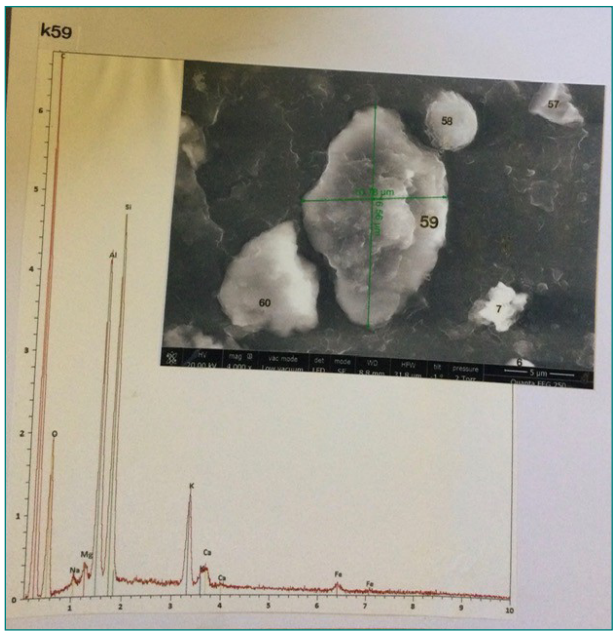

Figure 20. *The k59 particle. Above : SEM2 photograph (4000x), in LFD, of the lower part of the K area containing k59. Below : HR spectrum of k59.*

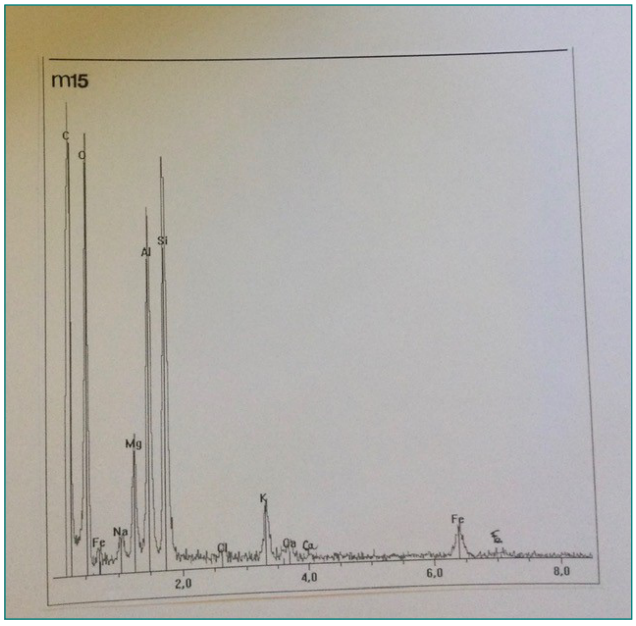

Figure 21. *The m15 spectrum*

Table 4. *List and characterization of the particles of the sixteen particles of potassium alumino-silicate with iron.*

Numbers	Nomenclature	Areas	Forms	Maximal lengths (in µm)	Potassium alumino-silicate spectras	Peculiarities	Colours
1	a24	A	triangular	13.5	+		not visible
2	b78	B	elongated	17.5	+	bipartite	yellow- red
3	d13	D	pentagonal	3.5	+		not visible
4	e113	E.e	Arqued	5	+	agglomerate of six sub- particles	red
5	j30	J	triangular	7.5	+		pale yellow
6	k59	K	elongated	10.8	+		yellow- red
7	l58		elongated	12.5	+		yellow-red
8	l64		hexagonal	14.5	+	bipartite	red
9	l72		elongated	6.5	+	titanium	pale yellow
10	m15		triangular	9.5	+		red
11	m54	M	losangic	5.5	+	bipartite	pale red

12	p6	P	rectangular	10	+		yellow
13	p10		elongated	9	+		yellow
14	p32		elongated	8.5	+		yellow-red
15	q17	Q	triangular	4.5	+	suddenly appeared on the Q area border	not- visible
16	r13	R	triangular	13.5	+		yellow-red

4. Discussion

Table 5 lists the particles and sub-particles of potential red colours that we detected in our studies. Their total number is of sixty eight, shared out in seven categories.

Nine of them are hematites. Hematite can be obtained by heating goethite (a clay), so hematite is an anthropic material. There is numerous evidence that hematite powders were used as red pigments, since Prehistory and beyond (1). Nine particles are biotites. All the observed biotite particles came from those of fine powders, pulverised and deposited on the TS surface; choice of these powders by operators was guided by the intention to obtain a special mica powder category (from the point of view of a finest powder) intensively red coloured. Being the heterogeneity (in shapes, iron oxide level and subtle differences in red-colour intensities) of the biotite particles observed, we can deduce that several sorts of such special mica-powder preparations were used (9) and that since the beginning of the Industrial Era.

Table 5. *List of the potentially red particles and sub-particles of seven categories detected on the triangle surface.*

Numbers	Materials	Particles and subparticles	Iron oxide	Mercury sulphure	Lead oxide	Products	References
1	hematites	l39, 07, b27, b28 and b28', b35, b36, b37, i14	+			anthropi c	Lucotte et al., 2016 and present study
2	biotites	i8, g34 and g34', j56, k70, k80, l8, l68, p53	+			anthropi c	Lucotte et al., 2016
3	cinnabar	k56		+		painting	Lucotte et al.,2016
4	iron-rich clays	a25, a27, a41, b8, b23, b24, b25, b26, g27, g30, g33, i4, j50, j51, l11, l34	+			mineral	Lucotte et al., 2024
5	particles of iron oxide	a5, "i1" and "i2", i61, j31, l70, p9, p19	+			anthropi c	present study
6	miniums	a5(1-7), j64, p37, p41, q6			+	painting	present study
7	particles of potassiu m alumino- silicate with iron	a24, b78, d13, e113, j30, k59, l58, l64, l72, m15, m54, p6, p10, p32, q17, r13	+			anthropi c	present study

There is only one cinnabar particle on the triangle surface. It is a paint-fragment of vermilion, a characteristic red coloured artist pigment that was commonly used in the Middle-Age (2). Its red colour was lightened with time.

Fifteen of these particles are iron-rich red clays (10). They are alumina-silicate clays, with an elevated content (up to 56%) of iron. Their colours are red or red-brown, depending on the iron content ; all these particles have a little quantity of the phosphorous element (up to 5%) in their compositions. The biggest ones show some morphological heterogeneity of their surfaces , suggesting that they are chipboards of some micro-organisms. This sort of clay is relatively specifics of the soils in the Middle-East region.

Eight of these particles are iron oxides. Five of them (a5, i61, l70, p9 and p19) are similar to McCrone balls (11). Study of a red ochre of reference (**Figure 22**) shows that it is a powder of such micro-balls, which spectras contain elevated iron contents. Red ochre was used as a red mineral pigment since the Prehistory.

Minium is a lead oxide that was used as a red artificial pigment since the Antiquity (it was obtained by heating ceruse). One formation and four particles of minium are detected on the triangle surface ; their red colours were lightened with time.

There are sixteen particles of potassium alumino-silcate with iron on the surface of the triangle. They represent heterogen products of modern constructions. Their red colour depend on their iron content.

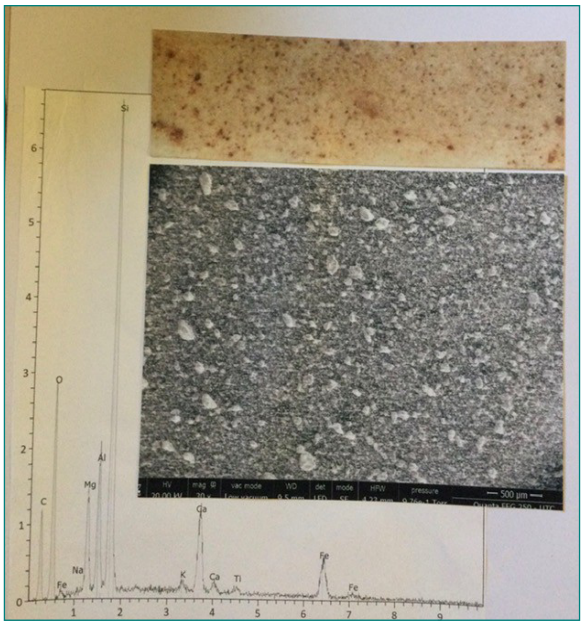

Figure 22. *Study of the modern red ochre of reference. Lower photograph : SEM2 photograph, in LFD, of some part of this ochre powder. Upper photograph : optical microscopy photograph of that part. Below : the global spectrum of the powder. Ti : titanium.*

Figure 23 shows the positions of the two red-coloured red blood cells and of the sixty-eight particles and sub-particles of potentially red colours on the triangle surface. There are no red particles on C, F, H, N and S areas. One particle is detected on areas D, E, O and R, two on areas M and Q, four in areas I and K, five in area G and six in areas J. Areas B, L and P are those with greatest quantities of red particles.

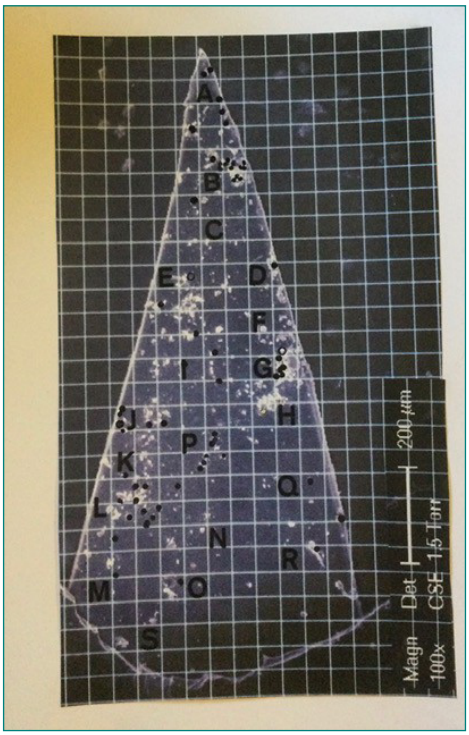

Figure 23. *Positions of the two red blood cells h19 and h22 and of the sixty- eight particles and sub-particles of potentially red colours on the different areas (A to S) of the triangle surface (little circles : h19 and h22 ; little black dots : the sixty-nine particles and sub-particles).*

To visualize the real red particles in one part of the triangle surface of great quantity of particles, **Figure 24** shows an optical microscopy photography of the (K)-L-(M) areas.

The l39 particle is an hematite. The l8 and l68 particles are biotites. The l11 particle is an iron-rich clay. The l70 particle is an iron oxide. The k59, l58, l64, l72 and m15 are particles of potassium alumino-silicate with iron and the l14, l17, l21 and l26 are brick micro-fragments.

But there are also more or less red in colours : the l34 particle is a calcium phosphate. The particles l40

(a calcite), l42 (a calcium carbonate), l46 (a red-brown Coccolith), l51-52-53 (another Coccolith), l56' (an orange calcium carbonate), l62 (a white and red marble micro-fragment), l65 (a brown Coccolith). Among the PVC plastics, l57 is a feuil with a red organic pigment. The l54 particle is a brown Diatom. The l7 particle is a red montmorillonite (Lucotte, 2023), specially iron-rich. All these last particles contribute also to the red colour of the L area.

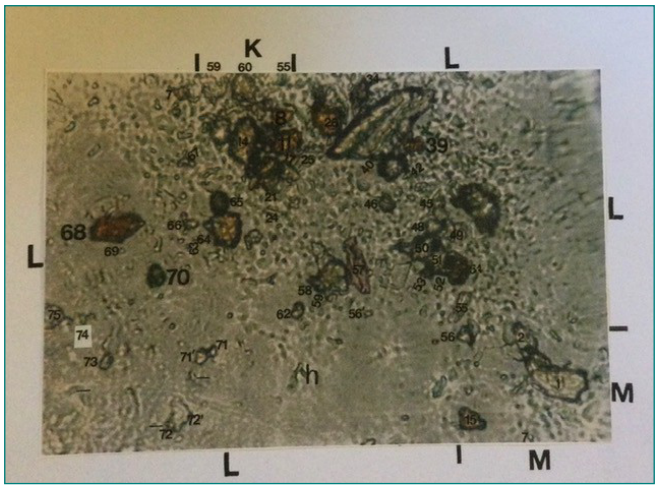

Figure 24. *Inverted optical microscopy photograph (1200x) of the L area of the triangle (including the lower part of the K area and the upper part of the M area). Particles on the L area are non-cited in the text are : l5 (a yellow calcite), l48 and l56 (two white calcium carbonates), l59 and l73 (two green PVC plastics), l66 and l67 (two yellow calcium carbonates), l69 (a white calcium carbonate), l71 (a white calcite). In the K area : k55 (a green plastic) and k60 (a yellow phospho-siderite). In the M area : m1 (a yellow feuil, with copper) and m2 (a little yellow feuil, with barium sulphure) : the m7 particle is a yellow clay. The three particles indicated by a dash are yellow or pale micro-balls of clays, previously undected ; h and l72' are holes.*

So I can explain – at least partialy – the red colour of the triangle. This red colour is mainly concentrated (**Figure 25**) at the limit between areas L and P of the triangle

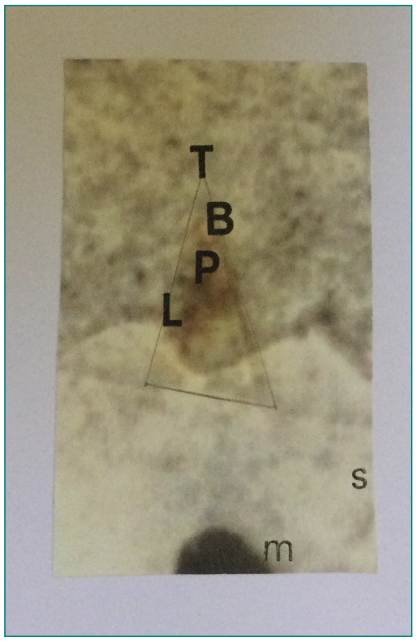

Figure 25. *Optical microscopy photograph (10x) of the triangle T (apex). S : sellotape ; m : black mark on the sellotape. B, P and L : approximate location areas (B : not red ; and P : limits) of the triangle.*

5. Conclusion

I have detected on the triangle surface, by SEM-EDX analyses, a total number of sixty-nine particles or sub-particles (nine hematites, nine biotites, one cinnabar, fifteen iron-rich clays, eight particles of iron oxides, eleven miniums, sixteen particles of potassium alumino silicates with iron) of potentially red colours. Among the twenty-five human red blood cells (or groups of human blood cells) founded on the triangle surface, only two of them are of red colours ; that is largely insufficient to explain the red colour of that surface.

I explain this red colour by the intentional addition during time to that surface of potentially red-coloured

products, one of them being mineral (iron-rich clays), four being anthropic (hematites, biotites, iron-oxide particles and particles of potassium alumina silicates with iron) and two being painting (cinnabar and miniums).

So the actual red colour of the Turin Shroud at the level of blood stains can be explained by some process of "reinforcement" by red artificial products of the faded red blood cells colour on this ancient linen tissue.

Conflict of Interest

The author declares no conficts of interest regarding the publication of this paper.

Acknowledgments

The author thanks T. Derouin (MNH of Paris) for his help in the optical microscopy studies, and S. Borensztajn (IPG of Paris) for his study of the minium sample of reference and T. Thomasset (UST of Compiègne) for SEM-EDX studies.

6. References

1. Cornell, R.M., Schwertmann, U. (1996). The Iron Oxides. VCH Verlagsgellschaft Ed., Weinheim, Germany.
2. Delamare, F., Guineau, B. (1999). Les matériaux de la couleur. Gallimard Ed., Paris, France.
3. Heller, J.H., Adler, A.D. (1980). Blood on the Shroud of Turin. *Applied Optics, 19*, 2742-2744.
4. Helller, J.H., Adler, A.D. (1981). A Chemical Investigation of the Shroud of Turin. *Canadian Society of Forensic Science of Journal, 14*, 81-103.
5. Kyropoulo, D., Dotsika, E. (2013). Stable Isotope Analysis as a Tool to Investigate Particulate Matter in Historic Libraries. *Preservation Science, 10*, 109-113.
6. Lucotte, G. (2015). Red Blood Cells on the Turin Shroud. *Jacobs Journal of Hematology, 2(1)*, 24-31.
7. Lucotte, G. (2017). The Triangle Project. *Newsletter of the British Society for the Turin Shroud, 85*, 5-14.
8. Lucotte, G. (2023). SEM-EDX Characterization of the Little Clays Particles Deposited on the Turin Shroud Surface. *Journal of Multidisciplinary Engineering Science and Techonlogy, 10 (4),* 15842-15847. (9) Lucotte, G., Derouin,T., Thomasset, T. (2016). Hematite, Biotite and Cinnabar on the Face of the Turin Shroud : Microscopy and SEM-EDX Analysis. *Open Journal of Apllied Sciences, 6*, 601-625.
9. Lucotte, G., Thomasset T., Derouin, T. (2024). Iron-Rich Red Clays on the Turin Shroud : Optical Microscopy Studies and SEM-EDX Analyses. *Archaeological Discovery, 12*, 66-81.
10. McCrone, W.C., Skirius, C. (1980). Light Microscopical Studies of the Turin Shroud. *Microscope, 28*, 105-112.
11. Petitfils, J.C. (2022). *Le Saint Suaire de Turin*. Tallandier Ed., Paris, France.